Impact of the time resolution for data gathering on loss calculation and demand side flexibility

# Impact of the Time Resolution for Data Gathering on Loss Calculation and Demand Side Flexibility

Gianfranco Chicco and Andrea Mazza
Dipartimento Energia "Galileo Ferraris"
Politecnico di Torino
Torino, Italy
gianfranco.chicco@polito.it, andrea.mazza@polito.it

***Abstract*— Accurate data metering is needed for enabling demand side flexibility and the related services. Sufficient resolution in time of the data gathered is essential to obtain detailed information on how consumers and prosumers use electricity. This paper addresses two specific points concerning the effects of the time resolution on (i) the estimation of the network losses, and (ii) the assessment of the average power peak magnitude and duration. Specific indicators are introduced to estimate the losses and assess the peak power based on the load pattern shape. These effects are analysed based on examples taken from real measurements. The results clearly show that the time resolutions used today (from 15 min to 1 hour) are insufficient to perform effective assessments oriented to enhance demand side flexibility. Interval metering with better resolutions (1 min or less) or innovative technologies such as event-driven energy metering should be used to provide significantly better solutions.**

***Keywords—Data management, losses, demand side flexibility, smart metering, interval metering, event-driven energy metering.***

## NOMENCLATURE

| | |
|---|---|
| $d_E$ | Euclidean distance |
| $m$, $M$ | Index and number of elementary time intervals |
| ref, r | (subscripts) Reference and reconstructed patterns |
| $t$ | Time |
| $z$ | Metering mode |
| $E$ | Equivalent voltage |
| $P$ | Load active power |
| $R$, $R_{max}$ | Equivalent resistance and its maximum value |
| $V$ | RMS voltage at the load terminals |
| $\Delta P$ | Active power losses |
| $\Delta W$ | Energy losses |
| $\chi$ | Sums of $P^2$ ratio |
| $\delta_1$, $\delta_2$ | Thresholds for event-driven energy metering |
| $\tau$ | Elementary time interval |
| $\psi$ | Network energy losses ratio |
| $\varsigma$ | Peak average power ratio |

## I. INTRODUCTION

### A. Motivation and Background

With the diffusion of a new generation of smart meters, huge amounts of data are potentially available on the load and generation power curves of producers, consumers and prosumers connected to the electrical networks. This availability poses key questions on which time resolution for data gathering is meaningful to obtain significant results.

The typical time steps used for interval metering (at regular rates of data acquisition) in various jurisdictions include 15 min, 30 min and 1 hour. These time steps have been used to perform clustering-based load profiling, aimed at forming distinct consumption classes [1-4]. Residential users are more challenging than other types of users [5], because their power patterns are rapidly changing and are highly dependent on consumers' lifestyle.

The European Union has recommended establishing a smart meter roadmap [6] to satisfy the requirements of the future markets. Among these requirements, the use of high-resolution time intervals and the definition of advanced architectures for the metering infrastructures, with high modularity and flexibility, are indicated.

### B. Relevant Literature and Regulatory Documents

The choice of the resolution in time, which determines the averaging time step, has a remarkable effect on the data that become available to study the operation of the grid. Solutions with interval metering at high resolution in time (10 min [7,8] or less, up to a few seconds for applications such as non-intrusive load monitoring [9,10]) have been used for local demand side applications, but are not available at the network level, mainly because of the large amount of data to be gathered, transmitted and elaborated.

In addition, schemes for data gathering different from interval metering, such as event-driven energy metering (EDM) [11,12], have been proposed as a viable and efficient way to characterise the power curves through measurements. EDM enhances the possibility to reconstruct the demand patterns, and in particular their peaks, with higher precision than in the traditional interval metering.

The establishment of the most convenient solutions for data gathering is one of the current challenges. The aspects to consider are many, ranging from technical aspects (linked to hardware requirements and to the burden on the communications channels) to economic aspects (linked to the costs of the equipment and of its deployment and management), as well as a number of further impacts on the quality of the services that can be provided by using these solutions. Many services are conceptualised under the notion of demand side flexibility (DSF) [13].

Several definitions of flexibility have been provided in the literature for generation and demand, also taking into account the presence of transmission and distribution networks [14]. A review of these definitions is outside the scope of this paper. Only one technical definition of flexibility is recalled here, taken from the Conclusion paper of the Council of European Energy Regulators [15]: "*Flexibility is the capacity of the electricity system to respond to changes that may affect the balance of supply and demand at all times*". From the demand side, an essential prerequisite for opening the possible deployment of DSF options is the availability of smart meters with suitable characteristics. However, the current generation of smart meters seems not to be sufficiently ready to support DSF in an effective way. The main reason is that the granularity in time could be too limited to reproduce the details of the load patterns needed to study DSF appropriately [13].

### C. Contributions and Organization

Author's post print – Editorial version with DOI: 10.1109/SEST48500.2020.9203295

This paper addresses in a novel and systematic way two particular aspects of the effects of the resolution in time:

1) The estimation of the network losses, depending in a non-linear way on the actual power flows, based on the load patterns measured at the supply points.
2) The identification of the timing and amplitude of the consumption peaks, which remarkably contributes to the DSF assessment.

Both aspects depend on the accuracy in the definition of the (net) load patterns [16]. In particular, if the load patterns are not determined in an appropriate way, the network losses could be incorrectly assessed. When dealing with network losses, the model of the distribution network is needed, with the corresponding parameters. However, in general the distribution network data are not available to the users. As such, a precise quantification of the possible impact on the network losses of using different time steps for interval metering cannot be carried out. For this purpose, Section II presents a new and simplified way to characterise this impact, by calculating the *sums of $P^2$ ratio*. Section III addresses how the identification of the demand peaks becomes more accurate for better resolution in time, at the expenses of the growth in the number of data to be managed. The analysis carried out in Section II and Section III is supported by examples taken from real measurements. The examples chosen are intentionally very simple, referring to single loads, to make it possible to focus on specific details and to highlight some basic concepts with a tutorial focus. However, the approach used is valid also for load patterns at higher level of aggregation, without loss of generality. Section IV contains the Conclusions.

## II. Preliminary Analysis for Different Time Steps with Euclidean Distances and Sums of $P^2$ Ratios

### A. Load pattern timings and reconstruction

Let us consider the data gathered for a single load, in a given period of observation. Let us denote as *elementary time interval* $\tau$ the shortest time step at which the data are available. All the other time steps are assumed to be multiple integers of the elementary time interval. The elementary time interval is chosen for load pattern analysis, and has no connection with the data sampling that occurs inside the meter to determine the active and reactive power. The average power pattern from interval metering with data gathered at $\tau$ = 1 s is considered as the *reference* average power pattern, and is taken here as the "true" power pattern for load analysis purposes. In practical applications to electrical networks, the interval metering time step for load pattern analysis is longer than 1 s.

In addition to interval metering, the EDM [11,12] alternative is considered. In EDM, the data gathering does no longer happen at regular time steps, but is based on a mechanism for the generation of events that depends on two user-defined thresholds:

a) The threshold $\delta_1$, which depends on the change of average power from one elementary time interval to the next one. The event is generated if this change exceeds the threshold.
b) The threshold $\delta_2$, set up on the accumulated energy variations. The average power variations at successive elementary time intervals are accumulated in time. The event is generated when the sum of these variations exceeds the threshold.

The thresholds can be adapted to represent the load pattern with different details.

For the sake of comparison among the load patterns, all the data are reported to the elementary time interval by considering constant values of the average power during the corresponding time step. In this way, it is possible to use a metric based on the Euclidean distance to compare the "true" load pattern with another load pattern reconstructed based on the one originated from another metering mode (e.g., interval metering with a given time step, or EDM with a given ($\delta_1$,$\delta_2$) pair) [17]. Let us consider a sequence of elementary time intervals $m = 1,\ldots, M$ inside the observation period. Let us further denote with $P([t_m-\tau, t_m])$ the average power of the "true" load pattern at elementary time interval $m$ and with $P_r^{(z)}([t_m-\tau, t_m])$ the average power at the same elementary time interval of the load pattern reconstructed from the initial data measured in the metering mode $z$. In all cases, the average power is determined after the elementary time interval has elapsed. The Euclidean distance is then formulated as:

$$d_E\left(P, P_r^{(z)}\right) = \sqrt{\frac{1}{M}\sum_{m=1}^{M}\left(P([t_m-\tau,t_m]) - P_r^{(z)}([t_m-\tau,t_m])\right)^2} \quad (1)$$

### B. Sums of $P^2$ ratio

Another way to assess the effectiveness of the load pattern representation is to construct a loss-oriented simple indicator. Let us consider the average active power data gathered in a given metering mode, and the corresponding load pattern reconstructed at time steps equal to the elementary time interval, as seen above. Let us assume that the load is supplied by a system represented with its Thevenin equivalent. For the sake of simplicity, let us assume a residential load supplied at low-voltage with given active power $P$. The supply cable has small cross-section, so that a pure resistance $R$ can be assumed to approximate the Thevenin impedance. Moreover, the reactive power of the load is null. In these conditions, taking the RMS voltage $V$ at the load terminals, the losses in the supply system are expressed in per units as $\Delta P^{(z)} = R\,P^2/V^2$. With a further approximation (that will be removed later) let us assume that the voltage is constant for any value of $P$ (practically neglecting the voltage drop in the Thevenin equivalent resistance). In this case, it is possible to formulate a very simple indicator as the ratio of the energy losses referring to a load pattern gathered in metering mode $z$ with the corresponding energy losses determined from the "true" load pattern. Let us call this new indicator "Sums of $P^2$ Ratio", denoted with the symbol $\chi^{(z)}$, with the following definition:

$$\chi^{(z)} = \frac{\sum_{m=1}^{M}\left(P_r^{(z)}([t_m-\tau,t_m])\right)^2}{\sum_{m=1}^{M}\left(P([t_m-\tau,t_m])\right)^2} \quad (2)$$

The rationale for the definition of this indicator is to find a simple way to understand the basic effects on the losses of using different time steps, using only the load patterns without depending on the characteristics of the supply system. Under the hypothesis of constant RMS voltage at

the load terminals, the (constant) resistance $R$ does not appear in the $\chi^{(z)}$ ratio.

Values of $\chi^{(z)}$close to unity indicate that the losses can be assessed in a way similar to what can be done from the "true" load pattern. However, values of $\chi^{(z)}$ lower than unity point out the presence of discrepancies in the assessment of the losses, in particular corresponding to an underestimation of the actual losses. This issue is very relevant, because the underestimation of the actual losses could cause an overestimation of the non-technical losses and an overdue alert on the need to search for the reasons of the occurrence of these non-technical losses.

*C. Accounting for network losses*

In order to assess whether the indicator $\chi^{(z)}$ may give a useful approximation of what happens in a supply line, the analysis has been extended to consider the Thevenin circuit that supplies the load pattern. Considering a single-phase low-voltage load, for the sake of simplicity the Thevenin equivalent impedance is taken as purely resistive. The Thevenin voltage $E$ is assumed to be the rated voltage (230 V). The resistance depends on the length of the supply line. For this purpose, the maximum resistance $R_{max}$ is calculated as the one that causes a voltage drop of 10% at the load supply point when the load takes the rated power (3 kW). Then, a dedicated analysis has been set up, by changing the resistance from 0 to $R_{max}$ in a regular way. For each elementary time interval, and for a given resistance $R$, the voltage $V$ at the load terminals is found by solving the equation $V^2 - E\,V + R\,P = 0$ for the reference load pattern, and the energy losses are calculated from the equation $\Delta W_{ref}^{(R)} = \tau\,R\,(P/V)^2$. For each reconstructed load pattern in the measuring mode $z$, the voltage $V$ at the load terminals is calculated with the equation $V^2 - E\,V + R\,P_r^{(z)} = 0$, then the energy losses are calculated as $\Delta W_r^{(R,z)} = \tau\,R\left(P_r^{(z)}/V\right)^2$. The *network energy losses ratio* $\psi^{(R,z)}$ is then calculated, for a given measuring mode $z$ and resistance $R$, as follows:

$$\psi^{(R,z)} = \frac{\sum_{m=1}^{M}\left(\Delta W_r^{(R,z)}([t_m-\tau,t_m])\right)}{\sum_{m=1}^{M}\left(\Delta W_{ref}^{(R)}([t_m-\tau,t_m])\right)} \qquad (3)$$

The comparison among the indicators $\psi^{(R,z)}$ and $\chi^{(z)}$ is useful to understand to what extent the results obtained with the sums of $P^2$ ratio, without knowing any data of the network, can represent situations in which the network energy losses are calculated using the network parameters.

*D. Tutorial example*

*D.1. Metering modes*

Let us consider the load pattern of a residential user [17]. The "true" load pattern is taken at the elementary time interval $\tau$ = 1 s, for one hour. The other metering modes are:

- *Interval metering* at different time steps. Some cases are shown with 1 hour, 30 min, 15 min, and 1 min time steps (Fig. 1). The first three values correspond to time steps used in the metering modes used for billing purposes, while the last one is shown as an example of shorter time step. For the calculations, a set of time steps has been selected in the range from one second to one hour, at multiples of 1 s, with the criterion that the total period of one hour can be exactly filled by the sequence of time steps. The 45 resulting time steps are reported in Table I, together with the number of points at which the average power are calculated.
- *EDM* with two different settings of the thresholds ($\delta_1$,$\delta_2$), namely, (i) $\delta_1$ = 200 W and $\delta_2$ = 50 Ws, resulting in 687 events (Fig. 2), and (ii) $\delta_1$ = 200 W and $\delta_2$ = 200 Ws, resulting in 57 events (Fig. 3).

The chosen load pattern is particularly challenging to represent, with the presence of both sudden peaks and fast variations. Some of these characteristics of the load pattern depend on the operation of a washing machine.

*D.2. Load pattern reconstruction and Euclidean distances*

In Fig. 1, Fig. 2 and Fig. 3, the "true" load patterns are superposed to the reconstructed load patterns. Actually, when the load pattern data are gathered in the interval metering or in the EDM modes, the "true" load patterns are not available. However, they are considered here for the sake of comparison. The "true" load pattern and the other load patterns have the same total energy in the hour of observation. From these figures, it appears clearly that the load pattern representation at relatively long time steps is rather ineffective. The quantification of the effectiveness in terms of quality of reproduction of the "true" load pattern is then carried out by using the Euclidean distance, while the new indicator $\chi^{(z)}$ quantifies, in a simplified and load pattern dependent-only way, the impact of the different time steps used in the metering modes on the supply system losses.

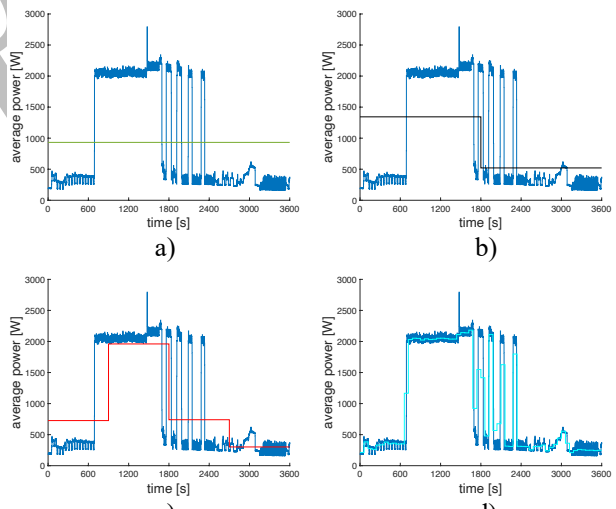


Fig. 1. Reference average power pattern from interval metering with data gathered at 1 s (blue line) and average power at 1 hour (a, green line), 30 min (b, black line), 15 min (c, red line) and 1 min (d, cyan line).

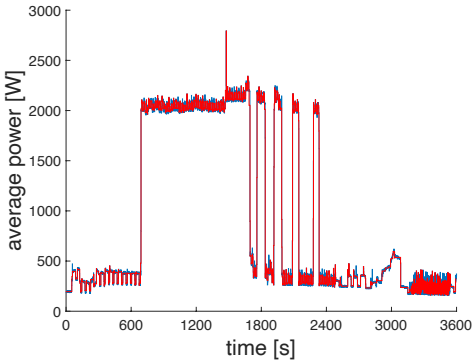

Fig. 2. Reference average power pattern from interval metering with data gathered at 1 s (blue line) and average power reconstructed from EDM with thresholds $\delta_1 = 200$ W and $\delta_2 = 50$ Ws (red line).

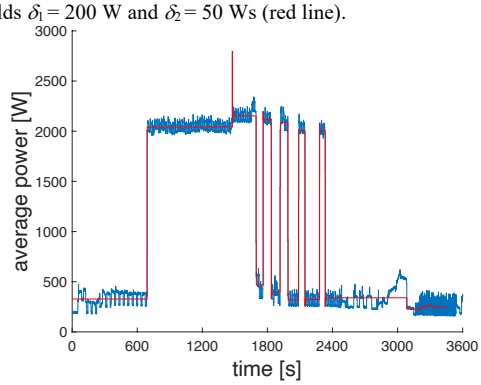


Fig. 3. Reference average power pattern from interval metering with data gathered at 1 s (blue line) and average power reconstructed from EDM with thresholds $\delta_1 = 200$ W and $\delta_2 = 200$ Ws (red line).

TABLE I.
SELECTED TIME STEPS IN ONE HOUR AND CORRESPONDING NUMBER OF POINTS AT WHICH THE AVERAGE POWER IS CALCULATED.

| Time step [s] | Number of points | Time step [s] | Number of points | Time step [s] | Number of points |
|---|---|---|---|---|---|
| 1 | 3600 | 25 | 144 | 150 | 24 |
| 2 | 1800 | 30 | 120 | 180 | 20 |
| 3 | 1200 | 36 | 100 | 200 | 18 |
| 4 | 900 | 40 | 90 | 225 | 16 |
| 5 | 720 | 45 | 80 | 240 | 15 |
| 6 | 600 | 48 | 75 | 300 | 12 |
| 8 | 450 | 50 | 72 | 360 | 10 |
| 9 | 400 | 60 | 60 | 400 | 9 |
| 10 | 360 | 72 | 50 | 450 | 8 |
| 12 | 300 | 75 | 48 | 600 | 6 |
| 15 | 240 | 80 | 45 | 720 | 5 |
| 16 | 225 | 90 | 40 | 900 | 4 |
| 18 | 200 | 100 | 36 | 1200 | 3 |
| 20 | 180 | 120 | 30 | 1800 | 2 |
| 24 | 150 | 144 | 25 | 3600 | 1 |

Fig. 4 shows the Euclidean distances calculated at the selected time steps. The trend is to obtain a higher Euclidean distance when the time step increases. Only the circled points are relevant, and the connecting lines only visualise the variation between points. However, this variation is non-monotonic, as it depends on the specific shape of the load pattern, which can be reproduced with different quality depending on the time step used. Fig. 5 contains a zoom of Fig. 4, focusing on short time steps and showing also the Euclidean distances calculated for the two cases with EDM.

In particular, it is possible to notice that the EDM cases are very effective in obtaining a load pattern reconstruction by using a number of points significantly lower than the interval metering cases. The case EDM(200,200) with 57 points (events) reaches an Euclidean distance as low as the one obtained with interval metering for time steps of 3 s (with 1200 points) or 4 s (with 900 points). From another point of view, the Euclidean distance in the EDM(200,200) case is 58.18 W, while in the interval metering with a comparable number of points (60 points, for time step of 1 min) the Euclidean distance is 279.77 W (the last point on the right side of Fig. 5). These results confirm the excellent behaviour of EDM, already noticed in many publications (e.g., [12,17]). If EDM is used with smaller threshold $\delta_2$ to capture more events, as in the EDM(200,50) case, the Euclidean distance is further reduced, reaching an effectiveness of "true" load pattern reproduction with 687 points better than what can be obtained with interval metering at time step of 2 seconds, with 1800 points.

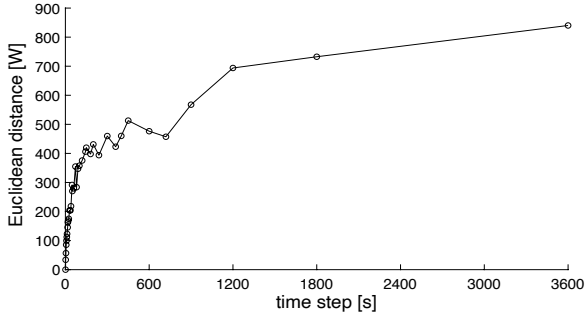


Fig. 4. Euclidean distances for the selected time steps.

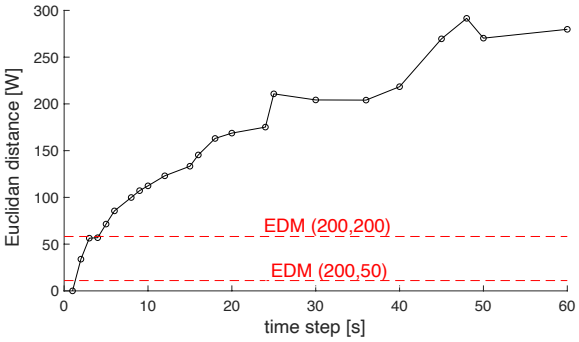


Fig. 5. Zoom of Fig. 4 with the two additional EDM cases.

It is also worth noting that the considered load pattern has many fluctuations with noticeable magnitude, while in more general cases (in particular for aggregated load patterns) the fluctuations have a lower magnitude, and the number of points resulting in the EDM cases are always much lower than the ones needed by interval metering to reach a performance comparable with EDM.

### *D.3. Calculation of the sums of $P^2$ ratios*

Fig. 6 reports the sums of $P^2$ ratio $\chi^{(z)}$ for the selected time steps with interval metering. The results clearly show that longer time steps generally cause a reduction of the indicator $\chi^{(z)}$. Again, the trend is not monotonic, due to the shape of the specific load pattern. An almost linear reduction of $\chi^{(z)}$ appears for relatively short time steps (Fig. 7). The salient result of this analysis is that the time steps currently used to gather load pattern data (from 15 minutes to 1 hour) are clearly insufficient to provide a reasonable representation of the energy losses. Large discrepancies could appear (the numerical outcomes depend on the specific load pattern). For the example shown, with interval metering the indicator $\chi^{(z)}$ is 0.795 for time step of 15 min, 0.6592 for time step of 30 min, and as low as 0.552 for time step of 1 hour. In the latter case, only about 55% of the energy losses could be estimated! Looking at Fig. 7, for the load pattern under analysis, with time steps not higher than 20 s it would be possible to estimate over 98% of the energy losses, and with the time step of 1 min it would be possible to estimate about 95% of the energy losses.

For the EDM cases, the situation becomes sensibly better. For $z$ = EDM(200,200), the indicator $\chi^{(z)}$ is 0.9954 with 57 points, while for $z$ = EDM(200,50) the indicator $\chi^{(z)}$ is 0.9983 with 687 points. Both values may represent a satisfactory estimation of the energy losses.

Furthermore, a high negative correlation has been found between the Euclidean distance and the indicator $\chi^{(z)}$, namely, with the correlation coefficient -0.953. This correlation provides a further confirmation of the conceptual soundness of using the indicator $\chi^{(z)}$ to mark the effectiveness of using shorter time steps both for better representing the load pattern and for how well the energy losses that can be found in the network may be estimated without knowing the network data. It has to be noticed that the high underestimation of the energy losses has been determined in a pattern with the larger variations mainly due to a single appliance. In a household there can be more appliances, and in a distribution feeder there are many customers. At more aggregate levels, generally the power patterns become smoother and the underestimation of the energy losses could be lower.

*D.4. Calculation of the network energy losses ratios*

Fig. 8 shows the results of calculating the indicator $\psi^{(R,z)}$ for different values of $R$ ranging from 0 to the maximum resistance $R_{max}$ determined as indicated in Section II.C, and for each measuring mode $z$. At each elementary time interval, the presence of the constant power load makes the calculation of the voltage at the load terminals non-linear. Furthermore, the energy losses change in a non-linear way with the voltage. The results from Fig. 8 are compared with the sums of $P^2$ ratios (black line), which conceptually corresponds to the case with $R = 0$. It can be seen that the network energy losses ratio is reduced when $R$ increases.

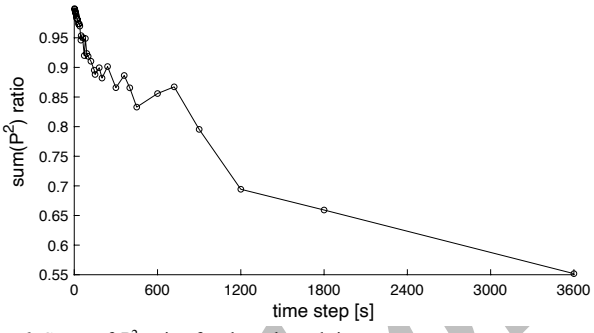


Fig. 6. Sums of $P^2$ ratios for the selected time steps.

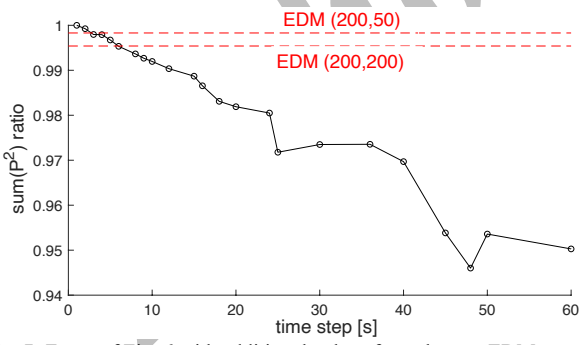


Fig. 7. Zoom of Fig. 6 with additional values from the two EDM cases.

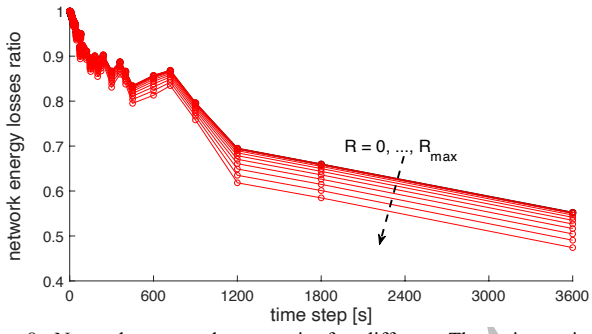


Fig. 8. Network energy losses ratio for different Thevenin equivalent resistances and load pattern averaging time steps for interval metering. Black line: sums of $P^2$ ratio; red lines: cases with different line resistances.

Hence, the sums of $P^2$ ratios can be considered a viable indicator of the network energy losses ratio, especially for relatively short lines that cause limited voltage drops. The representativeness of the energy losses becomes even more limited when the length of the line that supplies the same load increases. With hourly data, in the case analysed with resistance $R_{max}$, the indicator $\psi^{(R_{max},1\,hour)}$ falls below 0.5, thus representing very poor performance and possible misleading results provided to the operators.

## III. Flexibility and Demand Peaks

One of the significant points to analyse the demand flexibility is the capability to assess and represent the peaks that occur in the load patterns. For this purpose, the time step used for data gathering plays a fundamental role. In this section it is shown that the time steps currently used for billing purposes (e.g., 15 min, 30 min or 1 hour) can be totally ineffective to represent the demand peaks. The example considered is based on the same load pattern analysed in the previous section. For the purpose of identifying the actual peaks, the indicator used is the *peak average power ratio* $\varsigma^{(z)}$, defined by using the peak average power $\hat{P}$ found for the "true" load pattern as the reference value, the peak average power $\hat{P}_r^{(z)}$ of the load pattern reconstructed from the data gathered in metering mode $z$, and calculating the indicator as follows:

$$\varsigma^{(z)} = \frac{\hat{P}}{\hat{P}_r^{(z)}} \tag{4}$$

As it can be seen in Fig. 1, the reference average power pattern has a single peak occurring for a limited time. Fig. 9 shows the peak average power ratio for the interval metering with the selected time steps reported in Table I. As shown in the previous section for the related indicators, with the data considered no monotonic trend appears. The hourly time step is only able to represent the average power during one hour, and in this case the outcome is only about one third of the actual peak of the "true" load pattern. Also the use of 30 min time step reveals a peak lower than one half of the actual peak, and for 15 min time step only about 70% of the actual peak is reached. All these values are clearly unsatisfactory to be considered as a basis for any flexibility reasoning. Therefore, shorter time steps should be adopted. Fig. 10 shows a zoom of Fig. 9 limited to 1 min time step. It appears that even 1 min time step is not satisfactory, as only about 80% of the actual peak is represented. In the specific case, the time step with interval metering should be as low as 3 s to get the representation of over 90% of the actual peak. From interval metering, to reach the actual peak, only

time steps of 1 s or 2 s are appropriate. Of course, the results are data-driven and cannot be generalised. However, they are indicative of the peak power issue.

From Fig. 10, it is also evident that the use of the EDM alternatives becomes fully successful, as both cases reported, namely, EDM(200,200) and EDM(200,50), reach 100% of the actual peak.

The possibility of accurately identifying the actual peak is only one of the aspects that may be useful to assess the demand flexibility. More generally, a relevant point is the construction of the duration curves of the load patterns, which allow the data analyst extending the assessment of the overall shape of the load pattern [18].

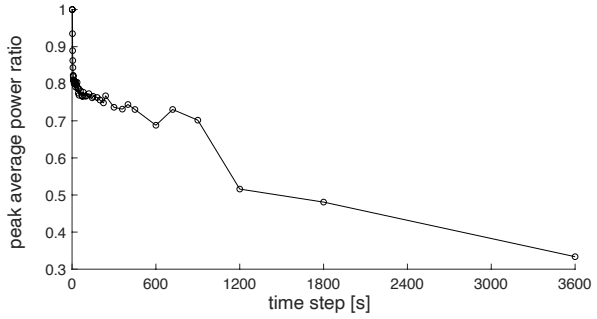


Fig. 9. Peak average power ratio for the selected time steps.

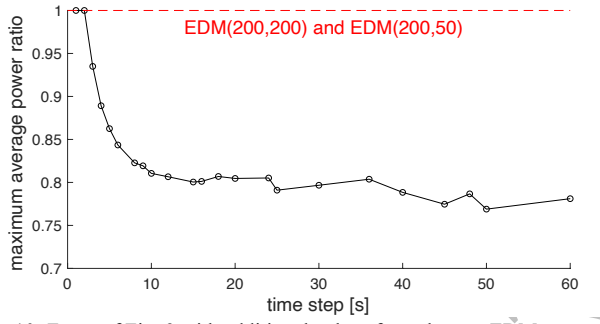


Fig. 10. Zoom of Fig. 9 with additional values from the two EDM cases.

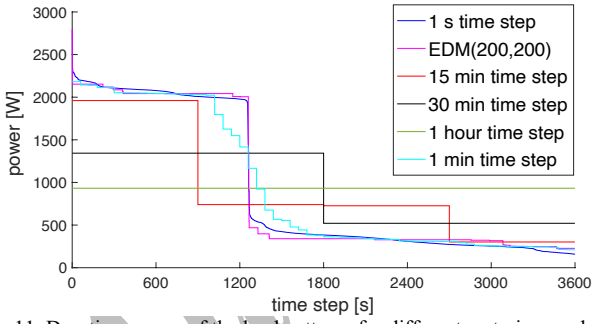


Fig. 11. Duration curves of the load patterns for different metering modes.

Fig. 11 shows the duration curves of the reconstructed load patterns. The most appropriate duration curves are close to the duration curve drawn with 1 s time step. Fig. 11 highlights the advantage of using EDM with respect to interval metering, also using EDM(200,200), which is less efficient than EDM(200,50) as shown above. With interval metering, even the case with 1 min time step would not be particularly effective with the data used in this example.

## IV. Conclusions

This paper has defined specific indicators to estimate the losses and assess the peak power based on load pattern data gathered with different metering modes. The residential load chosen for the examples of application is a challenging case with relevant pattern variations.

The results described in this paper clearly show that the estimation of the energy losses of the network, carried out by using data gathered at the time steps currently used (from 15 minutes to 1 hour) can be largely misleading. In fact, the actual losses can be highly underestimated (even to only 50%-70% of the losses calculated with the time step of 1 second). The underestimation could be lower in case of smoother power patterns, e.g., at higher levels of user aggregation. The sums of $P^2$ ratios, newly introduced in this paper, satisfactory estimates the network energy losses ratio, and can be used also when the characteristics of the distribution system that supplies the load are not known.

Likewise, the use of the data gathered at time steps from 15 minutes to 1 hour can be even worse to represent the demand peaks and the duration curves built from the load patterns. Therefore, for effective DSF assessment it is essential to reduce the time step of interval metering to values not yet adopted in the electrical networks. To avoid increasing the number of data managed, a successful alternative is the adoption of EDM with appropriate settings of the two related thresholds. Adaptive thresholds, variable in time, may also be used. The thresholds settings can be identified through an experimental campaign with measurements gathered at different load aggregation levels.

## V. References


[1] R. Li, F. Li and N.D. Smith, "Multi-Resolution Load Profile Clustering for Smart Metering Data," *IEEE Trans. on Power Systems*, vol. 31(6), pp. 4473-4482, 2016.

[2] G. Le Ray and P. Pinson, "Online adaptive clustering algorithm for load profiling," *Sustainable Energy, Grids and Networks*, vol. 17, art. 100181, 2019.

[3] S. Lin, F. Li, E. Tian, Y. Fu and D. Li, "Clustering Load Profiles for Demand Response Applications," *IEEE Trans. on Smart Grid*, vol. 10, no. 2, pp. 1599-1607, March 2019.

[4] G. Chicco, D. Labate, A. Notaristefano, and F. Piglione, "Unveil the Shape: Data Analytics for Extracting Knowledge from Smart Meters", *Energia Elettrica Supplement Journal*, vol. 96(6), 2019, DOI: 10.36156/ENERGIA06_01.

[5] T. Cerquitelli, G. Chicco, E. Di Corso, *et al.*, "Clustering-based assessment of residential consumers from hourly-metered data", *International Conference on Smart Energy Systems and Technologies (SEST 2018)*, Seville, Spain, 10-12 September 2018.

[6] European Smart Grids Task Force - Expert Group 3, Demand Side Flexibility - Perceived barriers and proposed recommendations, Final Report, April 2019.

[7] A. Albert and R. Rajagopal, "Smart Meter Driven Segmentation: What Your Consumption Says About You", *IEEE Trans. on Power Systems*, vol. 28(4), pp. 4019-4030, 2013.

[8] F. Luo, W. Kong, G. Ranzi, and Z.Y. Dong, "Optimal Home Energy Management System with Demand Charge Tariff and Appliance Operational Dependencies", *IEEE Trans. on Smart Grid*, vol. 11(1), pp. 4–14, 2020.

[9] M.A. Devlin and B.P. Hayes, "Non-Intrusive Load Monitoring and Classification of Activities of Daily Living Using Residential Smart Meter Data", *IEEE Trans. on Consumer Electronics*, vol. 65(3), pp. 339-348, 2019.

[10] M. Xia, W. Liu, K. Wang, W. Song, C. Chen, and Y. Li, "Non-intrusive load disaggregation based on composite deep long short-term memory network", *Expert Systems with Applications*, vol. 160, art. 113669, 2020.

[11] M. Simonov, "Hybrid scheme of electricity metering in Smart Grid", *IEEE Systems Journal*, vol. 8(2), pp. 422–429, 2014.

[12] M. Simonov, G. Chicco, and G. Zanetto, "Event-Driven Energy Metering: Principles and Applications", *IEEE Trans. on Industry Applications*, 53(4), pp. 3217–3227, 2017.

[13] Council of European Energy Regulators, CEER Advice on Ensuring Market and Regulatory Arrangements help deliver Demand-Side Flexibility, Ref: C14-SDE-40-03, 26 June 2014.

[14] P. Grunewald and M. Diakonova, "Flexibility, dynamism and diversity in energy supply and demand: A critical review", *Energy Research & Social Science*, vol. 38, pp. 58–66, 2018.
[15] Council of European Energy Regulators, CEER Distribution Systems Working Group, Flexibility Use at Distribution Level - A CEER Conclusions Paper, C18-DS-42-04, 17 July 2018.
[16] G. Chicco and A. Mazza, "Understanding the Value of Net Metering Outcomes for Different Averaging Time Steps", *3rd International Conference SEST 2020*, Istanbul, Turkey, 7-9 Sept. 2020.
[17] M. Simonov, G. Chicco, S. Ferro, and G. Zanetto, "Knowledge extraction from event-driven metering of electrical consumption patterns", *Proc. PSCC 2016*, Genoa, Italy, 20-24 June 2016, vol. 1, pp. 497–503.
[18] G. Chicco and A. Mazza, "New insights for setting up contractual options for demand side flexibility", *Journal of Engineering Sciences and Innovation*, vol. 4(4), pp. 381-398, 2019.